SP-423

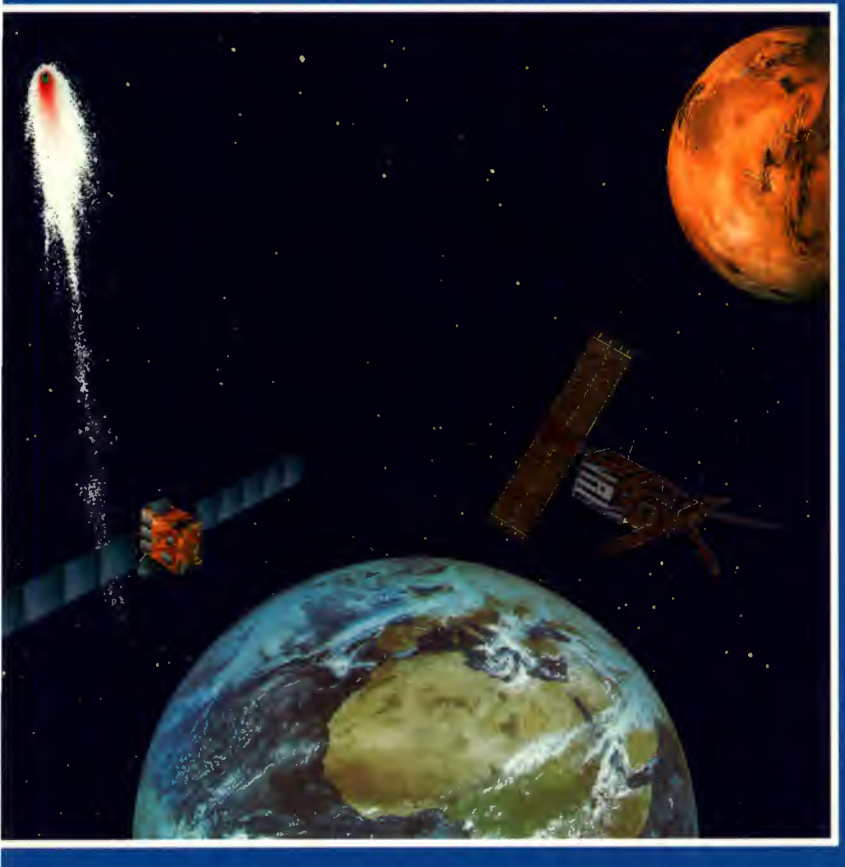

The 32nd ESLAB Symposium on

Remote Sensing Methodology for Earth Observation and Planetary Exploration

ESTEC, Noordwijk, The Netherlands
15-18 September 1998

European Space Agency
Agence spatiale européenne

LOW NOISE FAR-INFRARED DETECTION AT 90 K USING HIGH-T_C SUPERCONDUCTING BOLOMETERS WITH SILICON-NITRIDE BEAM SUSPENSION

M.P. Bruijn, M.J.M.E. de Nivelle, P.A.J. de Korte
Space Research Organization Netherlands, Utrecht, The Netherlands

S. Sánchez, M. Elwenspoek
MESA Research Institute, Enschede, The Netherlands

T. Heidenblut, B. Schwierzi
Institut für Halbleitertechnologie und Werkstoffe der Elektrotechnik, Hannover, Germany

W. Michalke, E. Steinbeiss
Institut für Physikalische Hochtechnologie, Jena, Germany.

ABSTRACT

High-T_c $GdBa_2Cu_3O_{7-\delta}$ (GBCO) superconducting transition edge bolometers with operating temperatures near 90 K and receiving area of 1 mm^2 have been made with both closed silicon-nitride membranes and patterned silicon-nitride (Si_xN_y) spiderweb-like suspension structures. To enable epitaxial growth of the GBCO layer, a thin monocrystalline Si layer is prepared on the silicon-nitride base, using fusion bonding techniques. By pattering the silicon-nitride supporting membrane the thermal conductance G is reduced from 20 to 3.5 μW/K. The noise of both types of bolometers is fully dominated by the intrinsic noise from phonon fluctuations in the thermal conductance G. The optical efficiency in the far infrared is about 75% due to a gold black absorption layer. The optical noise equivalent power (NEP) is 1.8 pW/√Hz, and the detectivity D^* is 5.4×10^{10} cm√Hz/W. Time constants are 0.1 and 0.6 s, for the closed membrane and the spiderweb like bolometers respectively. We have observed an empirical limit for the NEP for this type of bolometers. The effective timeconstant can be reduced with a factor of 3 by using an electronic feedback system or by using voltage bias. A further reduction necessarily results in an increase of the NEP due to the $1/f$ noise of the superconductor.

1. INTRODUCTION

Detection of far-infrared radiation (wavelength between roughly 30 and 300 μm) is an important driver for definition of space-based scientific missions. Far-infrared radiation is emitted by relatively cool objects in space, like planets and interstellar dust clouds. Because of absorption in the earth's atmosphere, observation must be done from space. Observation of these very faint structures requires the use of detectors with the highest possible sensitivity. Thermal detectors and photovoltaic (photon) detectors at temperatures below 10 K are normally the primary choice. For a review, see Richards (1994). For investigation of chemical processes in the earth's atmosphere, detection of far-infrared radiation plays an important role as well. Hydroxyl radicals (OH) for instance play a role in the catalytic cycles, that control the stratospheric ozone budget: the most important Odd-Hydrogen cycle and the NO_x and ClO_x cycles (Wennberg et al. 1994). The OH radical can be discriminated from other players in these cycles most easily in the far-infrared part of the spectrum (Chance et al. 1994). Because of the higher radiation levels, compared to space astronomy, less sensitive detectors can be of use. This enables the use of higher operating temperatures, which require less complicated, light weight and low power consuming cooling facilities. At liquid nitrogen temperatures, thermal detectors posses a better performance for detection of far-infrared radiation than doped Si or Ge photon detectors (Richards 1994).

Amongst the thermal detectors, high-T_c transition edge bolometers are the most promising. The very sharp resistance change enables changes in temperature to be detected with high sensitivity. During the last few years, much effort has been put into development of this type of detector (Verghese et al. 1993, Richards 1994, Brasunas & Lakew 1994, Johnson et al. 1994, Berkowitz et al. 1996, Méchin et al. 1997). Members of the present collaboration have been involved in this development since 1995, starting with bolometers on Si-membranes (Neff et al. 1995). Soon thereafter the noise equivalent power (NEP) was improved by one order of magnitude by replacing the Si-membrane by a silicon-nitride supporting layer (at the cost of time contant) (de Nivelle et al. 1997). Bolometers from this development will be flown on a balloon mission SFINX (Hoogeveen 1997). The present work aimed at further improvement of the detectivity $D^*=\sqrt{Area/NEP}$ by exploiting the limits of reduction of the thermal conductance G through the use of larger membranes and structuring of the supporting membrane (like the "spiderweb" bolometers of Bock et al. 1995). Furthermore the reduction of timeconstant was investigated (theoretically) by the use of other biasing schemes than regular current bias.

Proc. 32nd ESLAB Symp., 'Remote Sensing Methodology for Earth Observation and Planetary Exploration', ESTEC, Noordwijk, The Netherlands, 15-18 September 1998 (ESA SP-423, December 1998)

In this publication we describe the results obtained with three different types of high-T_c bolometers. The first type contains a closed SiN membrane, but now with a larger membrane size. The two other types are bolometers with a patterned SiN membrane resulting in eight SiN beams suspending the sensing area of the membrane with a remaining foil of PtO_x between these beams, and bolometers without this foil which have completely freestanding SiN legs.

2. PRODUCTION TECHNOLOGY

The fabrication process of bolometers with a closed silicon-nitride membrane was described before by Sánchez et al. (1998). The present fabrication processes form an extension of this process. The processes of the bolometers with patterned membranes is illustrated in Figure 1. From the various routes that were investigated, two routes are presented here. The first part of both routes is the same.

The starting substrate is a so-called silicon-on-nitride (SON) wafer. The SON wafers are made by bond-and-etch-back of two wafers: A commercially available silicon-on insulator (SOI) wafer from SOITEC and a Si wafer on which a 1 μm silicon-rich silicon-nitride ("SiN") layer has been grown. Previous to the bonding the SiN is chemically-mechanically polished (CMP), using a standard procedure from integrated circuit planarisation technology. Si and SiO_2 from the SOI wafer is removed by wet etching. The SiN layer at the backside of the Si wafer is used as a mask for etching the membrane windows. The etching is stopped when the SiN membrane is still supported by about 25 μm of Si. The resulting membranes are strong enough for the following processes.

The next step is epitaxial growth of a 40 nm double bufferlayer of yttrium stabilized zirconia (YSZ) and CeO_2 on the Si top layer using molecular beam epitaxy. The layer growth is monitored in-situ using low energy electron diffraction (LEED). Then the meander pattern for the high-T_c layer is etched in the bufferlayers and the Si layer by argon sputter etching and reactive ion etching (RIE) respectively. This step will define the area of the GBCO layer that will be superconducting (inhibition patterning). A second resist mask is used to define the suspension beams in the SiN layer. Etching is done by RIE. It is stopped when there is about 250 nm SiN left between the suspension beams.

From this point on the two routes will differ. The substrates are diced into pieces of 1×1 cm^2. In route a) (see Figure 1) the GBCO layer is deposited by hollow magnetron sputtering. On top of the GBCO a passivation layer of 200 nm platinum oxide (PtO_x) is deposited by planar magnetron sputtering. Then, using a special designed protection holder, which seals off the front side of the substrates, the remaining 25 μm of Si is removed

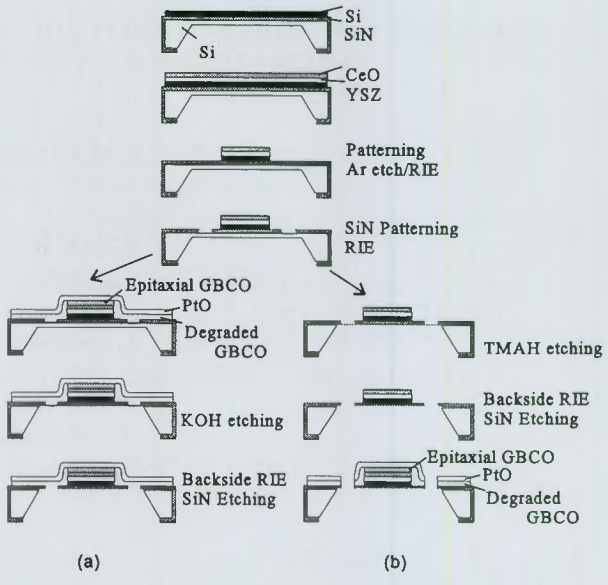

Figure 1. Schematic overview of the production routes of HTS bolometers. The individual process steps are clarified in the text. Route a) results in bolometers with a foil of degraded GBCO and PtO_x between the suspension legs. Route b) results in freestanding spiderweb-like bolometers.

from the backside of the membranes by KOH etching. The 250 nm thick SiN layer between the beams of the web structure prevent the KOH from reaching the front side. This SiN layer can be removed by RIE. The resulting bolometers have a remaining GBCO/PtO_x layer between the SiN beams. This GBCO is degraded and will not become superconducting. To get rid of the GBCO/PtO_x between the SiN beams it is required to follow route b): The Si at the backside of the membrane and the 250 nm of SiN between the beams have to be removed before deposition of the GBCO.

Finally on top of the bolometers an absorption layer of gold-black is deposited through a shadow mask with a pinhole of 1.1 mm diameter. The thickness is between 25 and 50 micrometer, with a filling fraction of 0.003. The resulting absorption efficiency for radiation with wavelengths around 100 μm is approximately 90% (Becker 1996).
Figure 2 shows a photograph of the backside of a bolometer with 8 SiN supsension beams and 60+200 nm GBCO/PtO_x between the beams. The PtO_x is buckling due to its compressive stress. In the center of the bolometer the superconducting meander can be seen through the SiN layer. In Figure 3 a bolometer is shown with really free-standing SiN beams, prepared along route b) in Figure 1.

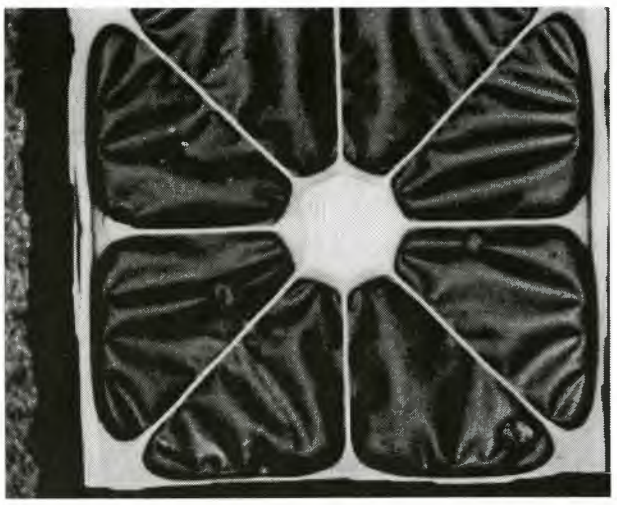

Figure 2. Photograph of the backside of a bolometer with a 4.5x4.5 mm membrane size. Between the 8 SiN suspension beams the residual layer of GBCO/PtO$_x$ can be seen, which is buckling due to its compressive stress. The beams are 40 μm wide and 1.6 or 2.2 mm long.

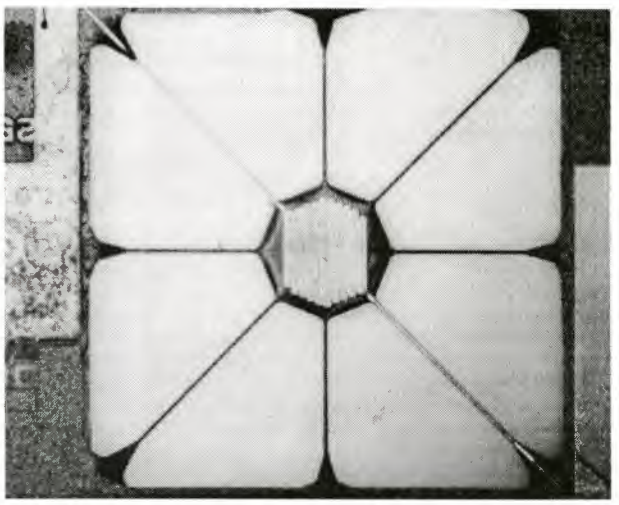

Figure 3. Photograph of a bolometer with freestanding SiN beams. The dimensions are the same as in Figure 2.

3. BOLOMETER PERFORMANCE

The bolometers were characterized in a vacuum cryostat with liquid nitrogen cooling. The bolometer temperature can be controlled with temperature fluctuations smaller than 5 μK (on a timescale of 100 s). The normal operating mode is current biasing. To reduce the low frequency noise of the electronics, a square wave current modulation at 1 kHz was used together with phase sensitive amplification.

3.1. Resistance vs Temperature Measurements

The thermal conductance G was detemined by measuring the superconducting transition at different current levels, and fitting the R-T_m curves on top of each other. Here $T_m = T_s + (I^2R+P)/G$ is the calculated temperature of the membrane, T_s is the temperature of the substrate and P is the radiation load on the bolometer. The results for the bolometer shown in Figure 2 are given in Figure 4. It was found that G=3.5 μW/K. The power load P could be neglected during this measurement. The normalised slope of the transition $\alpha = 1/R\ dR/dT$ at the point where the slope is at maximum is 1.1 K^{-1}. For all bolometers typically values between 1 and 2.5 K^{-1} were found.

An overview of the specifications of three typical bolometers with different geometries including the parameters R_{mid}, T_{mid} and α_{mid}, is given in Table 1. The subscript *mid* indicates the midpoint in the transition where the slope is at maximum.

The bolometer of Figure 3 was only tested sofar in a cryostat with unknown and high radiation load. The R-T measurement showed a superconducting transition,

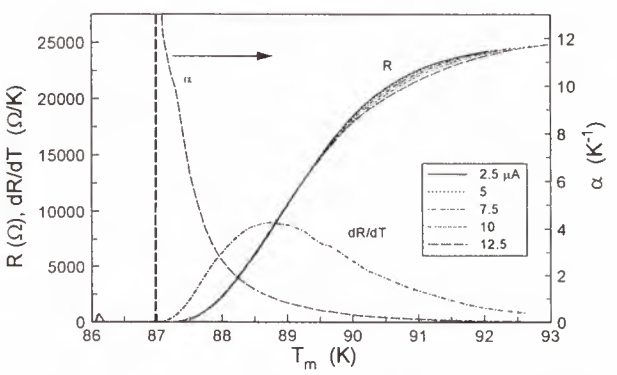

Figure 4. Resistance R, derivative dR/dT and normalized slope α as a function of the calculated membrane temperature $T_m = T_s + I^2R/G$ of the bolometer, shown in Figure 2. The value of G=3.5 μW/K was fitted from measurements at different bias currents I. R is plotted for the different bias currents between 2.5 and 12.5 μA.

indicating the feasibility of this production route, but the data was unsufficient reliable to be incorporated in Table 1. The yield of fabrication of bolometers along route b) (Figure 1) was largely enhanced by removal of half of the top Si-layer by oxidation followed by wet chemical etching of the oxide. Presumably the top part of the Si-layer contained damage that prevented growth of high quality buffer layers and high T_c layers.

3.2. Optical Responsivity

The absolute optical response of the bolometers has been determined with two radiation sources with different power levels. The sources were black bodies at 30 and 50 °C. Their radiation was filtered with a well-characterized filter at a temperature of 90 K and then collected on the bolometers with a compound parabolical concentrator (CPC or "Winston cone"). The resulting spectrum covers

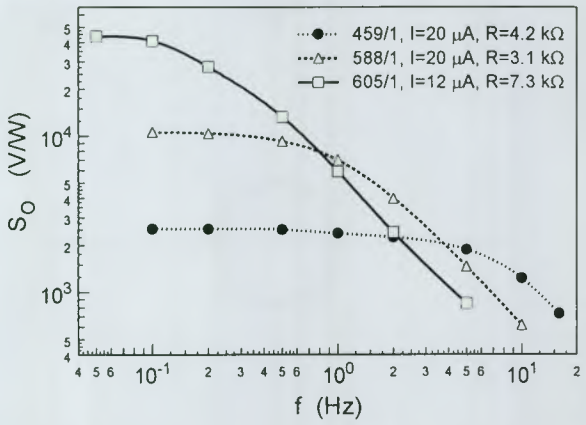

Figure 5. Measured optical responsivity of the three bolometers listed in Table 1. as a function of the signal frequency for radiation around 100 μm wavelength. The bias points are indicated in the figure. The boxes (605/1) represent the bolometer of Figure 2.

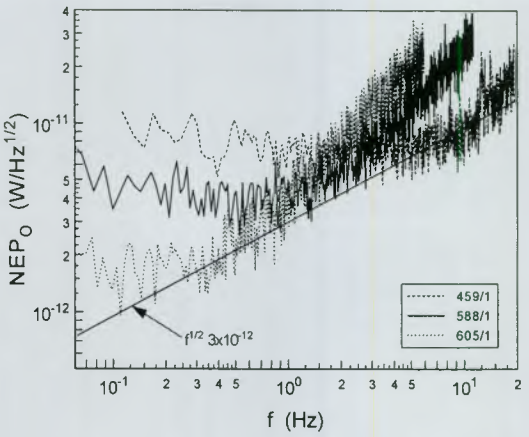

Figure 6. Measured NEP spectra of the three bolometers listed in Table 1. for radiation around 100 μm wavelength. The dashed data represent the one with 2x2 mm closed membrane. The solid line represents the one with 4x4 mm closed membrane and the dotted data belong to the spiderweb bolometer (Figure 2).
The straight line indicates the observed limit: $NEP_O=3x10^{-12}\sqrt{f}$ W/√Hz.

a band with wavelengths from about 70 to 200 μm with a maximum at 85 μm.

The frequency roll off of the bolometer was determined by measuring the response to a modulated light emitting diode. Figure 5 shows the resulting response spectra at indicated bias points of the three bolometers listed in Table 1. By comparing the measured optical reponse with the electrically determined responsivity we could conclude that the efficiency of the bolometers in the test setup is between 0.7 and 0.8. Careful analysis of the effects of defocussing at the exit opening of the CPC and the temperature gradient over the membrane indicate a true absorption efficiency of the detector close to 0.9, a value that can be calculated for the gold black absorption layer.

3.3. Noise Equivalent Power & Detectivity

The noise equivalent power (NEP) was determined by dividing the noise spectra by the optical responsivity. The result for the three bolometers is shown in Figure 6. For all bolometers there is a range of bias temperatures and bias currents for which the NEP spectra are similar and for which the NEP is minimal. Usually the current and the temperature can be chosen such that R is around R_{mid} and the bias parameter $L_0=I^2R\alpha/G$ is between 0.1 and 0.3. In the frequency range where the NEP is constant the NEP is dominated by the phonon noise in the thermal conductance G. The observed levels are in agreement with the theoretical level for the phonon noise given by:

$$NEP_{phonon} = \frac{\sqrt{4kT^2G}}{\eta} \qquad (1)$$

in which η is the optical absorption efficiency.
In Figure 6 a line is drawn which represents the experimental limit for the NEP of these bolometers. This limit $NEP_{limit} \approx 3\times10^{-12}\sqrt{f}$ W/√Hz. By decreasing the thermal conductance of the bolometers the NEP becomes smaller while at the same the bolometers become slower. The limiting relation between the NEP and the frequency

Table 1. Overview of the performance of three typical bolometers with different geometries.

#	R_{mid} (kΩ)	T_{mid} (K)	α_{mid} (K^{-1})	G (μW/K)	τ (s)	η	NEP_O ($pW/Hz^{1/2}$)	D^* ($cmHz^{1/2}/W$)	f (Hz)	Description
459/1	3.4	87.6	2	45	0.03	0.7	6.9	$1.4x10^{10}$	0.7-5	2x2mm² closed membrane
588/1	8.0	90.2	1.5	20	0.14	0.75	3.8	$2.6x10^{10}$	0.4-0.6	4x4mm² closed membrane
605/1	8.0	88.7	1.1	3.5	0.55	0.80	1.8	$5.4x10^{10}$	0.09-0.3	4.5x4.5mm² spiderweb (Figure 2)

is determined by the heat capacities of the bolometers which are all roughly 2 μJ/K. This can be seen by substituting for G in formula (1) the relation $G=C/\tau \approx 2\pi fC$. Formula (1) transforms into:

$$NEP_{phonon} \approx \frac{\sqrt{8\pi f\, kT^2 C}}{\eta} \qquad (2)$$

C could be made smaller by reducing the thickness of Au-black, PtO_x, Si or Si_xN_y. Reducing the Au thickness will cause the efficiency to decrease. The PtO_x is needed for protection against environmental attack. Reducing the Si thickness could be done by oxidation and etch back. The relative gain is only small. The only way is reducing the nitride thickness. This will cause the bolometers to become more fragile. We have not explored the limit in nitride thickness.

Another way to improve the NEP is by reducing the operating temperature. This also causes C to decrease. The problem is to find a suitable material with lower T_c and good noise properties. The aim of this route would be to fill in the gap between liquid-He cooled detectors and liquid-N_2 cooled high-T_c detectors, where cryocoolers can be used.

It has been argued that by using voltage bias with strong electrothermal feedback the effective timeconstant of the bolometers can be decreased (Mather 1982, Irwin 1995). Consequently, by reducing the thermal conductance the NEP can be decreased, while keeping the effective speed of the bolometer constant. Also biasing schemes can be designed in which a feedback loop reduces the fluctuations of the bolometer resistance by electrically compensating variations in the power of absorbed radiation. Thereby temperature excursions are reduced and the response speed is increased.

However, an unexpected noise term prevents this strategy to be effective with high-T_c bolometers: The $1/f$ noise. When electrothermal feedback is taken properly into account, the Johnson and $1/f$ noise can be written as (De Nivelle et al. 1997):

$$NEP_{Johnson} = \frac{1}{\eta}\sqrt{\frac{4kTG}{\alpha L_0}}\,|1+i\omega\tau| \qquad (3)$$

and

$$NEP_{1/f} = \frac{1}{\eta}\sqrt{\frac{\gamma_H 2\pi}{n_c E\omega}\,\frac{G}{\alpha}}\,|1+i\omega\tau| \qquad (4)$$

in which γ_H is the Hooge parameter (Hooge 1981), n_c the number of charge carriers and E the volume of the film. These formulae are independent of the biasing scheme. Using voltage bias, the loopgain L_0 can be made large because --unlike with current bias-- there is no limit set by the thermal runaway criterium. A large loopgain suppresses the NEP due to the Johnson noise, but the $1/f$ noise is not suppressed. At high frequencies, i.e. $\omega >> 1/\tau$, the NEP due to the $1/f$ noise becomes:

$$NEP_{1/f} = \frac{1}{\eta}\sqrt{\frac{\gamma_H f}{n_c E}\,\frac{2\pi C}{\alpha}} \qquad (5)$$

Typical values for our bolometers are: $\gamma_H = 1$, $n_c = 2\times10^{21}$ cm^{-3}, $E = 2.5\times10^{-8}$ cm^3, $C = 2$ μJ/K, $\alpha = 2$/K, $\eta = 0.75$. Substituting these values yields $NEP_{1/f} = 1.2\times10^{-12}\sqrt{f}$ W/√Hz.

Adding this in quadrature with the phonon noise, the minimum attainable NEP for our high-T_c bolometers at a given frequency, using voltage bias, will be $NEP_{limit} = 1.7\times10^{-12}\sqrt{f}$ W/√Hz. In terms of detectivity this can be expressed as $D^* = \sqrt{\text{Area}}/NEP = 1.5\times10^{11}\sqrt{\tau}$ cm√Hz/W. This is only a small improvement over the present limit with current bias. Alternatively, at a given NEP the device can only be made a factor 3 faster by using voltage bias.

4. CONCLUSIONS

By using a new technique to decrease the thermal conductivity, i.e. structuring the supporting membrane, we have developed high-T_c bolometers with an optical NEP of 1.8×10^{-12} W/√Hz at an operating temperature of 90 K. With the present technology we have approached the limit of the attainable detectivity at a given time constant of the device, and using current bias. These bolometers have the highest detectivity for time constants between 0.01 and 1 s, compared to those reported in present literature. The empirical limit in detectivity for bolometers on a 1 μm thick nitride membrane $D^* = 8.4\times10^{10}\sqrt{\tau}$ cm√Hz/W, when using current bias. Voltage bias will only result in improvement of detectivity with a factor 1.8, or time constant with a factor 3, compared to current bias, because of the effect of $1/f$ noise in the high-T_c films. The empirical limit for our bolometers in current bias is a factor 5 higher than Haven's empirical limit for room temperature thermal detectors (Rogatto 1993).

Really freestanding spiderweblike bolometers have been fabricated, but no conclusive data can be presented yet.

Shifting the limit for high-T_c bolometers further upward will require the heat capacity and/or the operating temperature to be lowered. We consider the feasibility of reduction of the thicknesses unlikely.

ACKNOWLEDGMENTS

Part of this work was performed under funding from the Earth Observation Preparatory Programme and the Technology Research Programme of the European Space Agency. The other part was financed by the Dutch Organization for Scientific Research (NWO).

REFERENCES

Becker W., Fettig R., Gaymann A., Ruppel W., 1996, Phys. Status Solidi B194, 241.

Berkowitz S.J., Hirahara A.S., Char K., Grossmann E.N., 1996, Appl. Phys. Lett. 69, 2125.

Bock J.J., Chen D., Mauskopf P.D., Lange A.E., 1995, Space Sci. Rev. 74, 229.

Brasunas J.C., Lakew B., 1994, Appl. Phys. Lett. 64(6), 777.

Chance K., Wijnbergen J.J., Schneider W., Burrows J.P., 1994, SPIE Proc. 2159, 21.

De Nivelle M.J.M.E., Bruijn M.P., De Vries R., Wijnbergen J.J., De Korte P.A.J., Sánchez S., Elwenspoek M., Heidenblut T., Schwierzi B., Michalke W., Steinbeiss E., 1997, J. Appl. Phys. 82(10), 4719.

Hooge F.N., Kleinpennig T.G.M., Vandamme L.K.J., 1981, Rep. Prog. Phys. 44, 479.

Hoogeveen R.W.M., Wijnbergen J.J., De Nivelle M.J.M.E., De Jonge A.R.W., Goede A.P.H., De Korte P.A.J., SPIE Proc. 3117, 19.

Irwin K.D., 1995, Appl. Phys. Lett. 66(15), 1998.

Johnson B.R., Foote M.C., Marsh H.A., Hunt B.D., 1994, SPIE Proc. 2267, 24.

Mather J.C., 1982, Appl. Opt. 21(6), 1125.

Méchin L., Villégier J.C., Bloyet D., 1997, J. Appl. Phys. 81, 7039.

Neff H., Laukemper J., Khrebtov I.A., Tkachenko A.D., Steinbeiss E., Michalke W., Burnus M., Heidenblut T., Hefle G., Schwierzi B., 1995, Appl. Phys. Lett. 66, 2421.

Richards P.L. 1994, J. Appl. Phys. 76(1), 1.

Rogatto W.D. (ed.), 1993, The Infrared & Electro-Optical Systems Handbook, Vol. 3, 204, copublished by Infrared Information Analysis Center & SPIE Optical Engineering Press.

Sánchez S., Elwenspoek M., Gui C., De Nivelle M.J.M.E., De Vries R., De, Korte P.A.J., Bruijn M.P., Wijnbergen J.J., Michalke W., Steinbeiss E., Heidenblut T., Schwierzi B., 1998, J. Microelectromechanical Syst. 7 (1), 62.

Verghese S., Richards P.L. Sachtjen S.A., Char K., 1993, J. Appl. Phys. 74, 4251.

Wennberg P.O., Cohen R.C., Stimpfle R.M., Koplow J.P., Anderson J.G., Salawitch R.J., Fahey D.W., Woodbridge E.L., Keim E.R., Gao R.S., Webster C.R., May R.D., Toohey D.W., Avallone L.M., Proffitt M.H., Loewenstein M., Podolske J.R., Chan K.R., Wofsy S.C., 1994, Science 266, 398.